12.810 Dynamics of the Atmosphere

E-P fluxes and instability in midlatitudes

Why do the transient eddies occur?

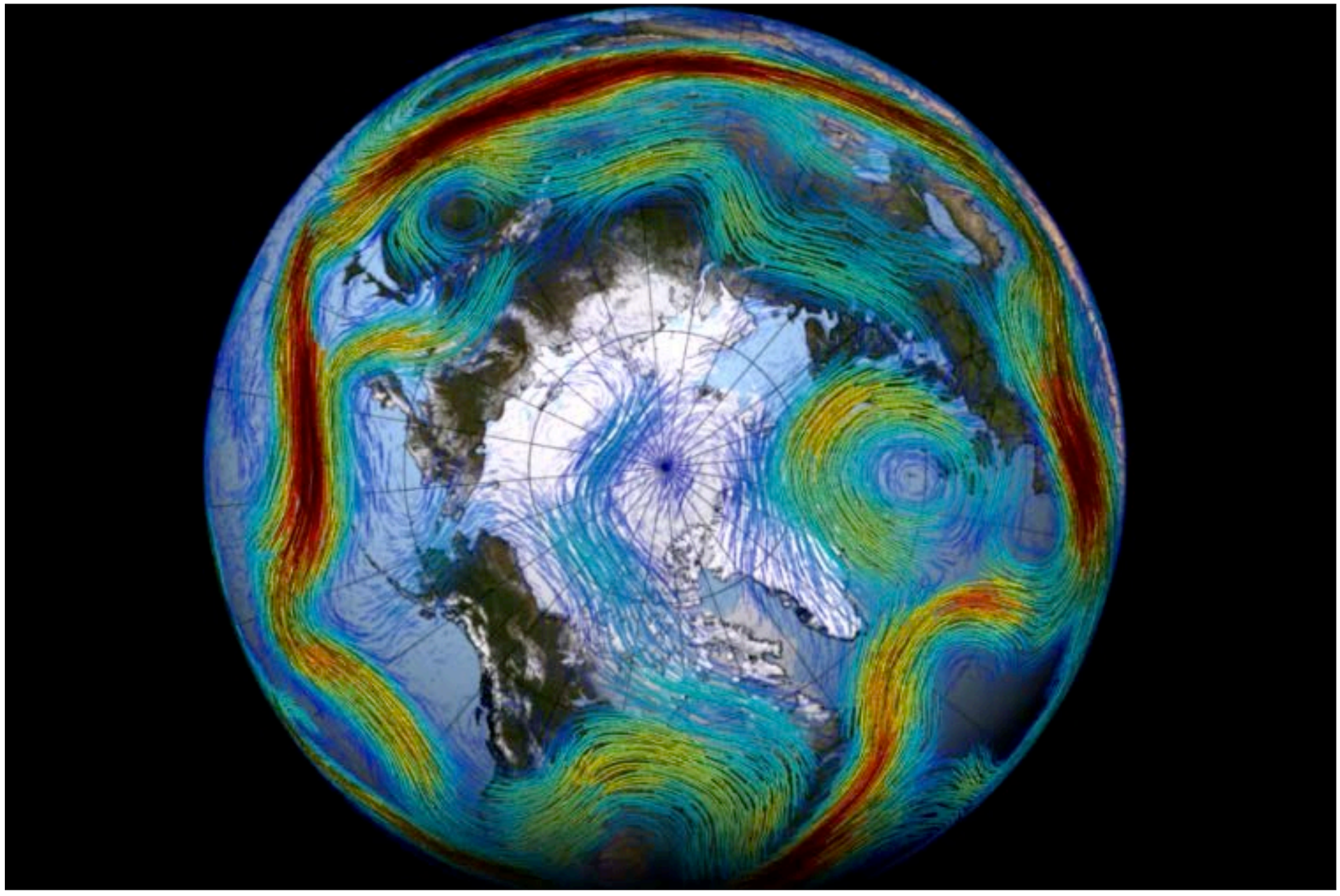

Upper level winds from June 10th to July 8th 1988 from MERRA
Red shows faster winds

https://svs.gsfc.nasa.gov/3864

Courtesy of NASA/Goddard Space Flight Center Scientific Visualization Studio.

Instability at midlatitudes

1. Fluxes of wave activity and the necessary condition for instability

2. Barotropic and baroclinic instability

3. The Eady model

Eliassen-Palm fluxes and their divergence: DJF

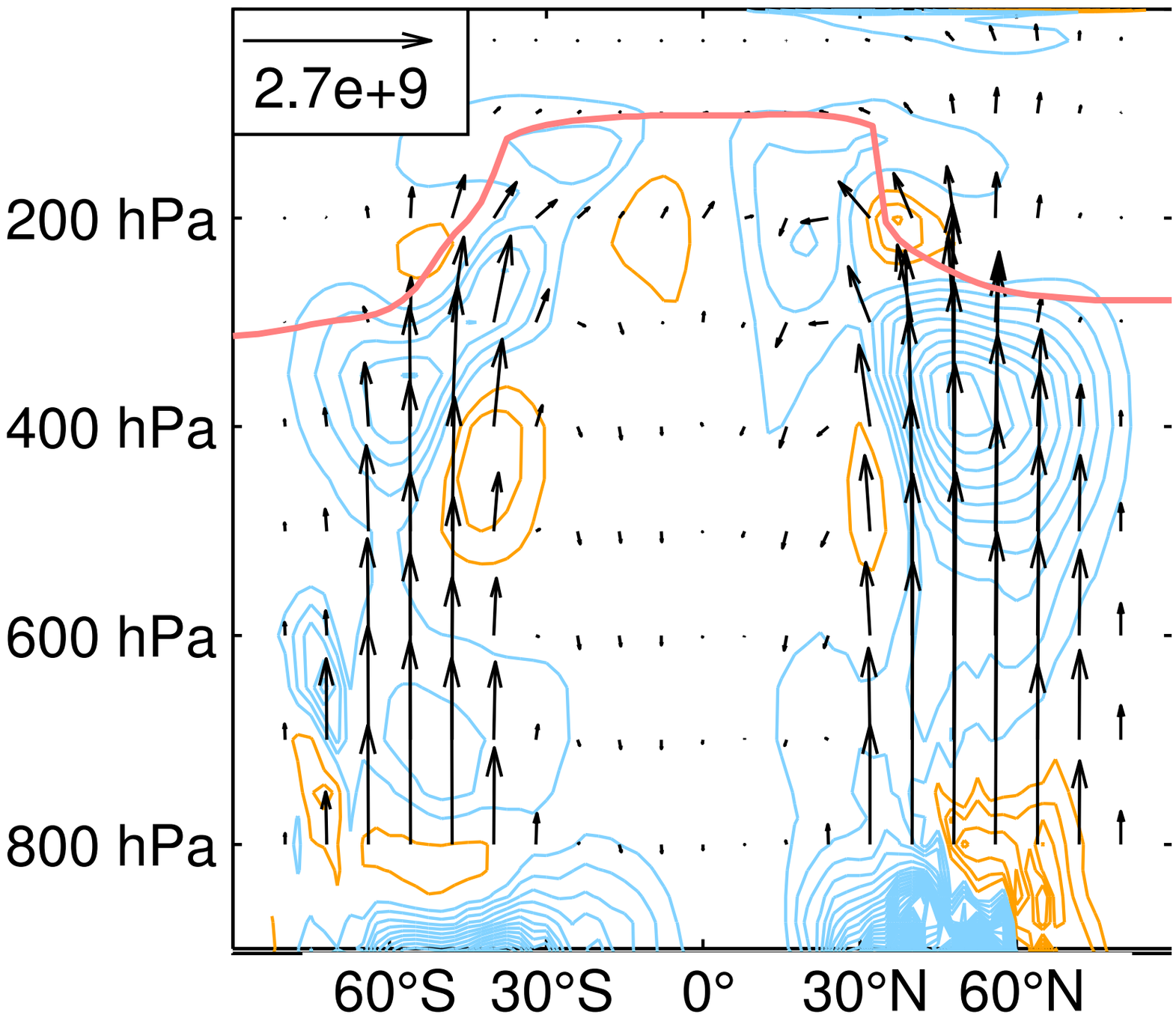

EP fluxes (arrows); orange is divergence, blue is convergence

The reference arrow has units m^3s^{-2}. The contour interval is 75 m^2s^{-2}.

Red line is the tropopause. Based on ERA-interim 1980-2013. Figure courtesy John Dwyer.

Fig. 1

Eliassen-Palm fluxes and their divergence: stationary eddies only (DJF and Northern Hemisphere)

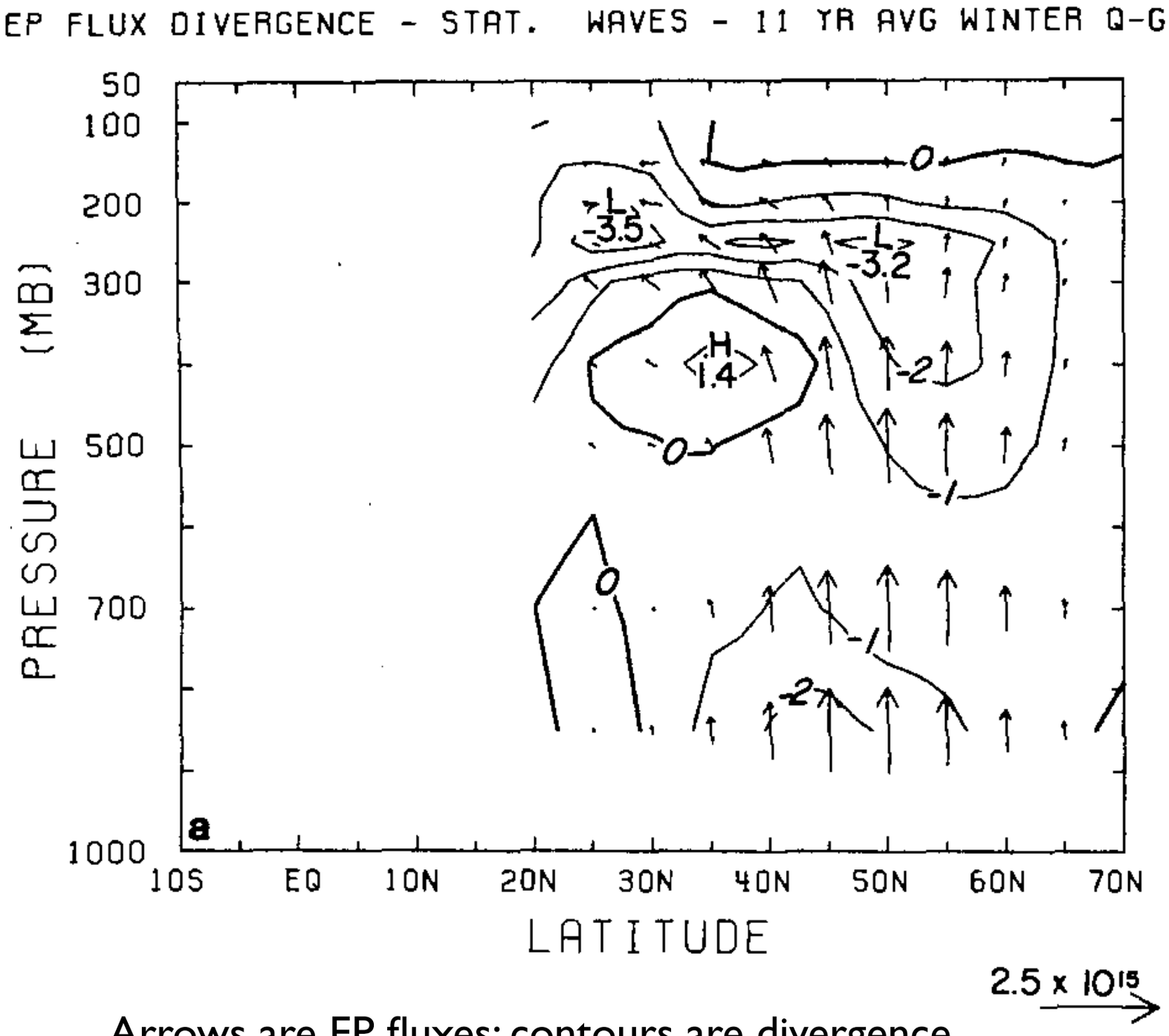

Arrows are EP fluxes; contours are divergence.

From Edmon et al 1980

Fig. 2

Instability of the African Easterly jet

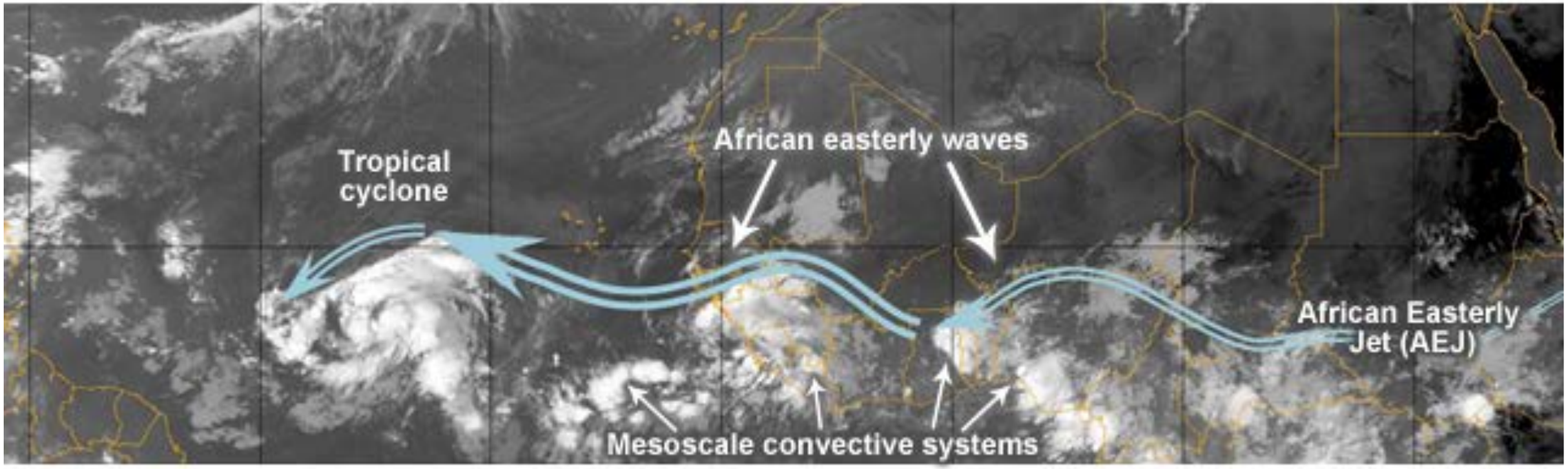

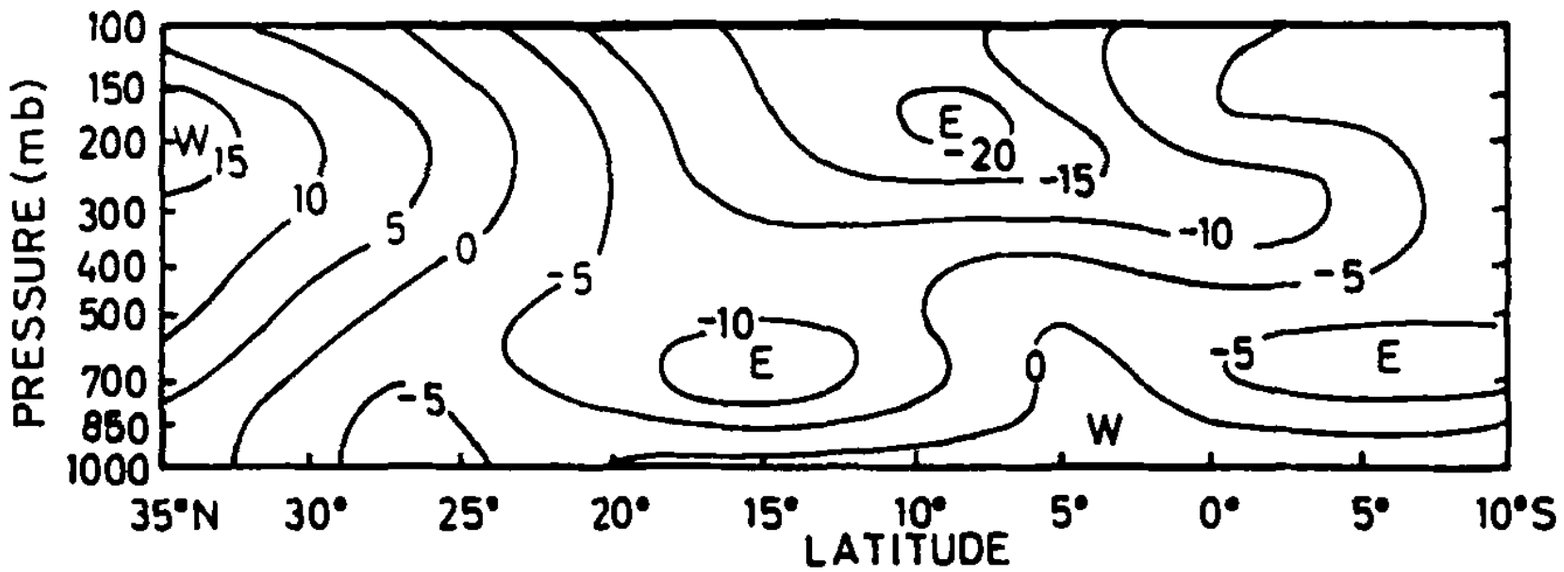

Fig. 3

Mean zonal wind at 5 degrees East in August
Hoskins & Thorncroft 1994

Easterly waves and tropical cyclones during 5–20 July 2005

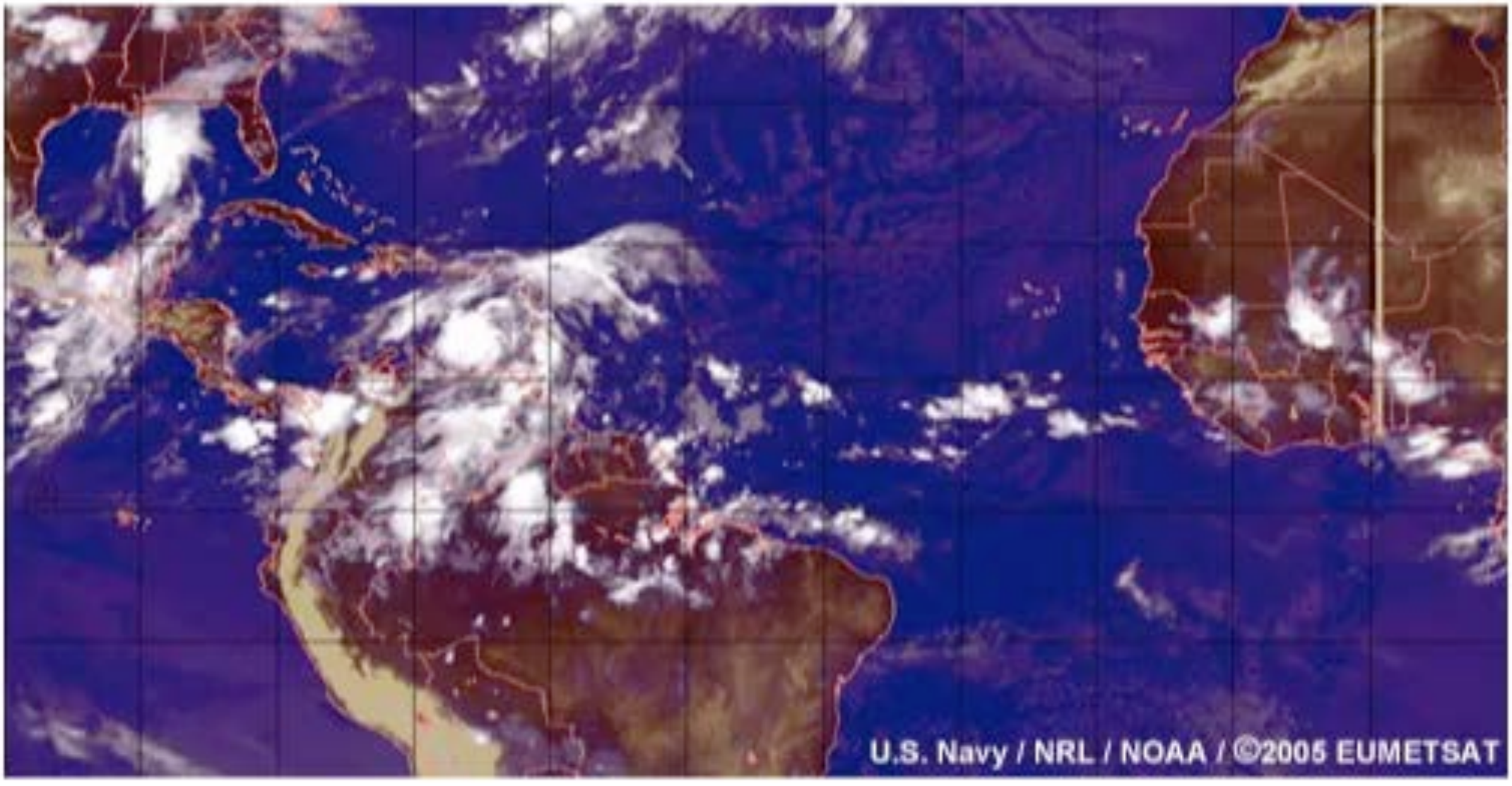

Fig. 3

Meridional PV gradient is negative here (red dashed line marks the Easterly jet)

Fig. 3

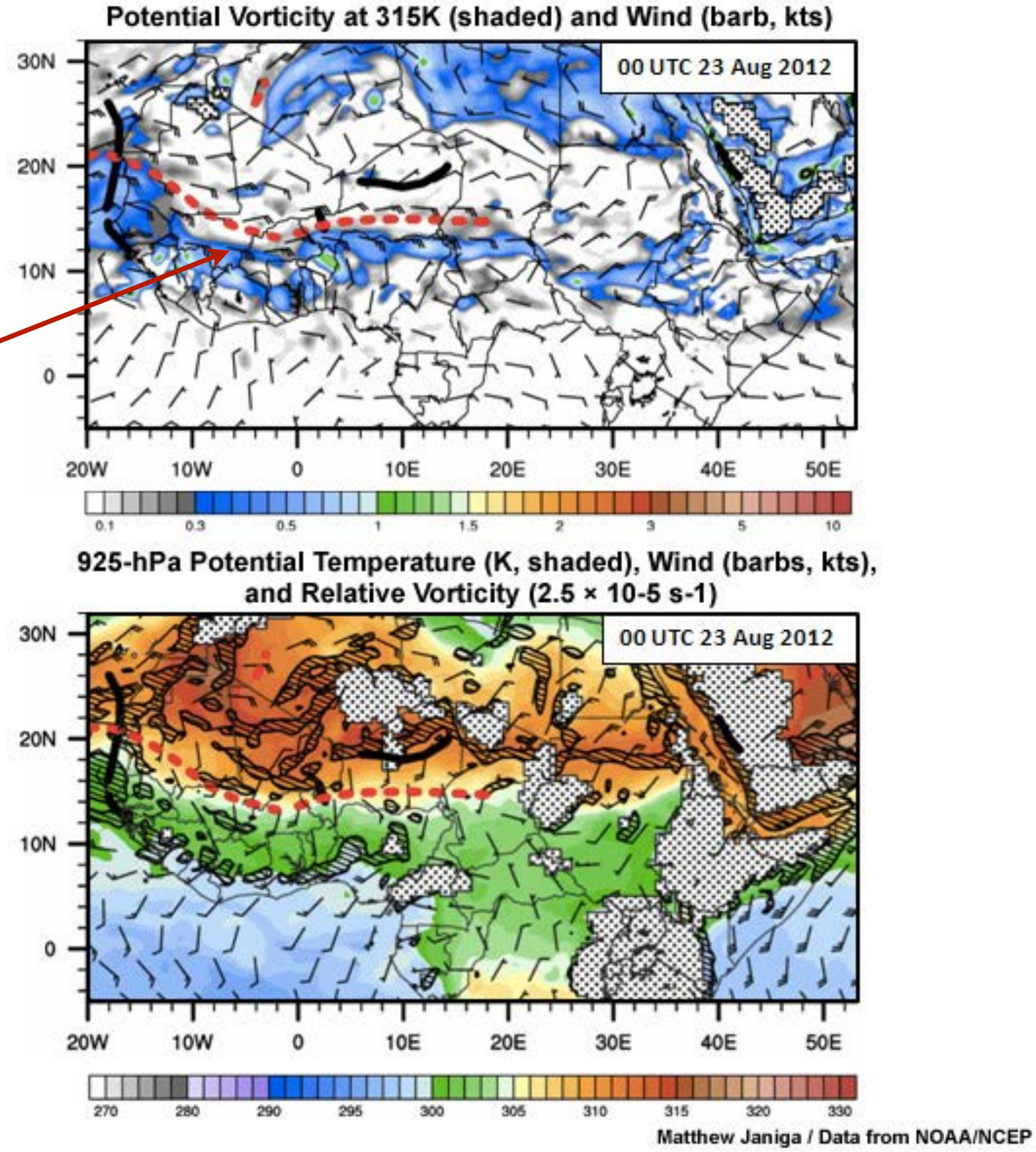

Image courtesy of Matthew Janiga. Used with permission.

Spinup of eddies in an idealized general circulation model (GCM)

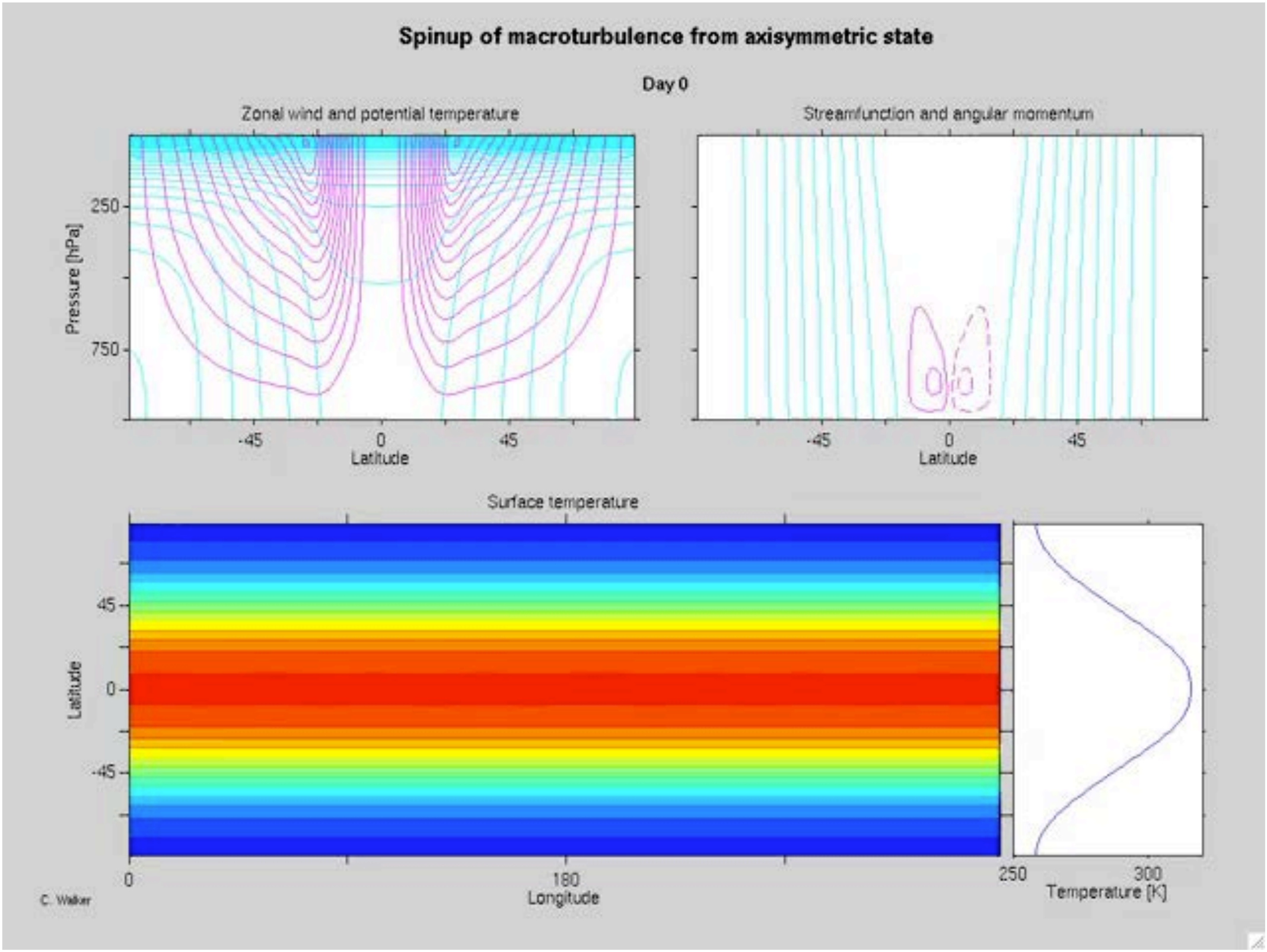

Fig. 4

Eady explains why he didn't include any references in his seminal paper on baroclinic instability!

A more detailed treatment of cyclone theory was given in a doctoral thesis (unpublished: London, 1948). The literature on cyclone and long wave theory is extensive and the writer would like to be excused the compilation of a list of references. He would however like to refer to an independent analysis by J. G. CHARNEY (Journal of Meteorology, Vol. 4, No. 5, Oct., 1947) which in many (but not all) respects is consistent with his own.

Eady, Tellus, 1949

Warm surface anomaly and associated cyclonic circulation

(contours are of potential temperature,
equivalent to buoyancy in the Eady model)

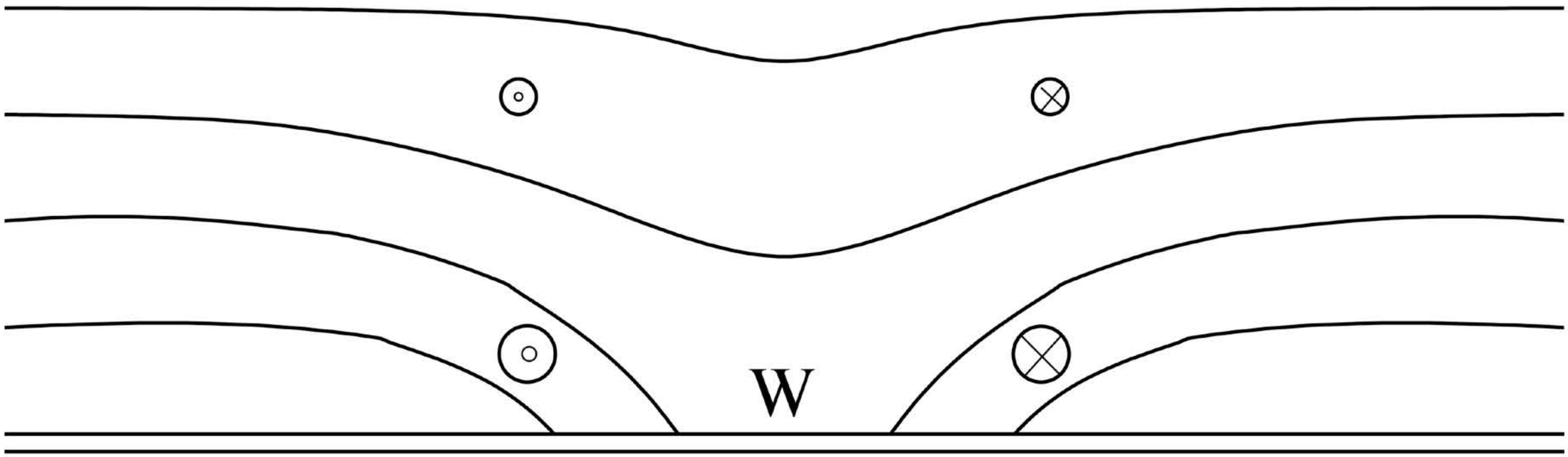

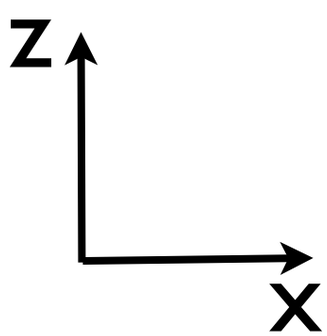

Fig. 5

Image courtesy of Glenn Flierl. Used with permission.

Looking down on warm surface anomaly with associated cyclonic circulation

(contours are of potential temperature, dashed show a later time, line with arrow shows the induced circulation)

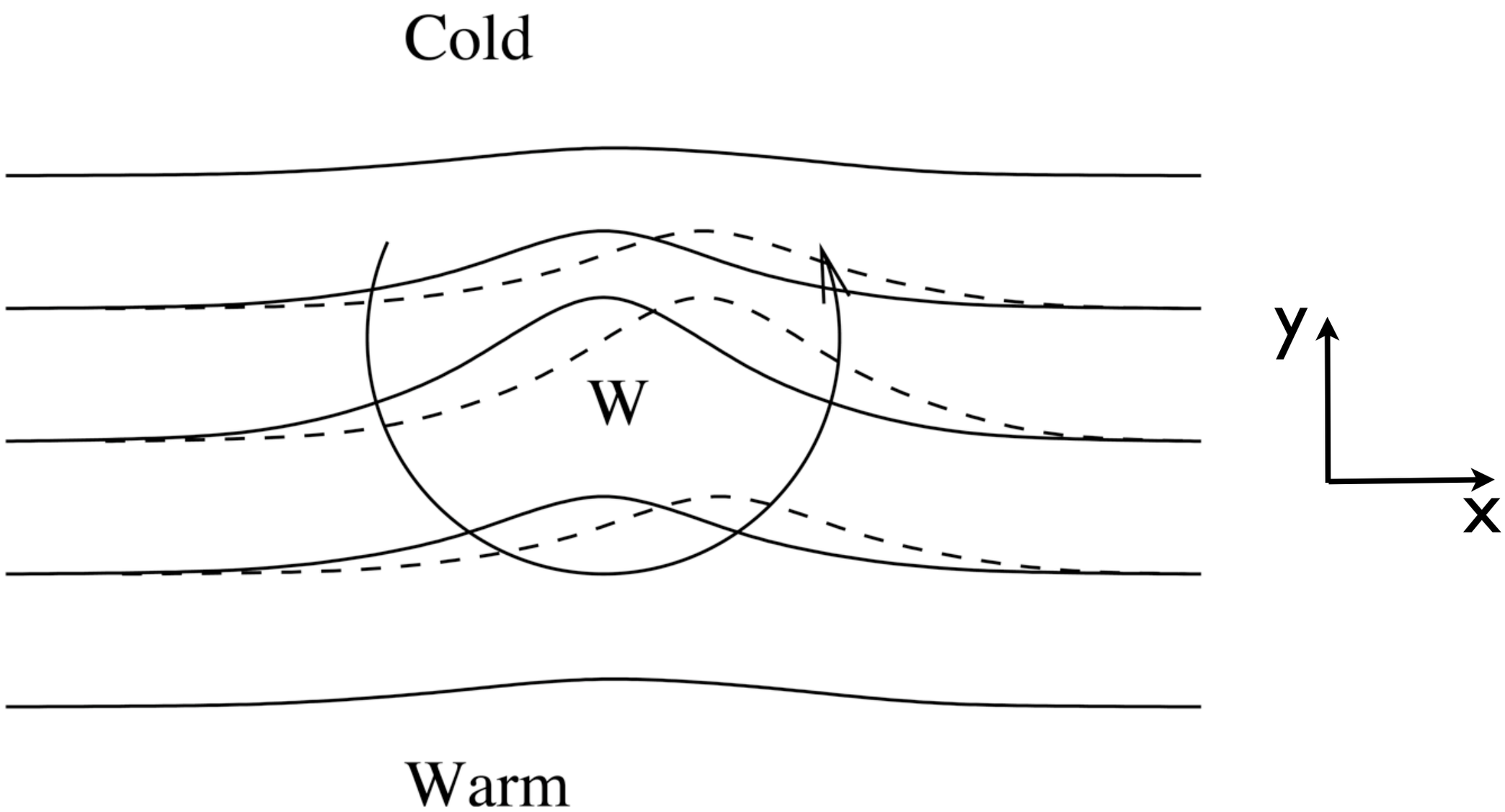

Fig. 6

The warm anomaly propagates eastward

Structure of a growing unstable mode

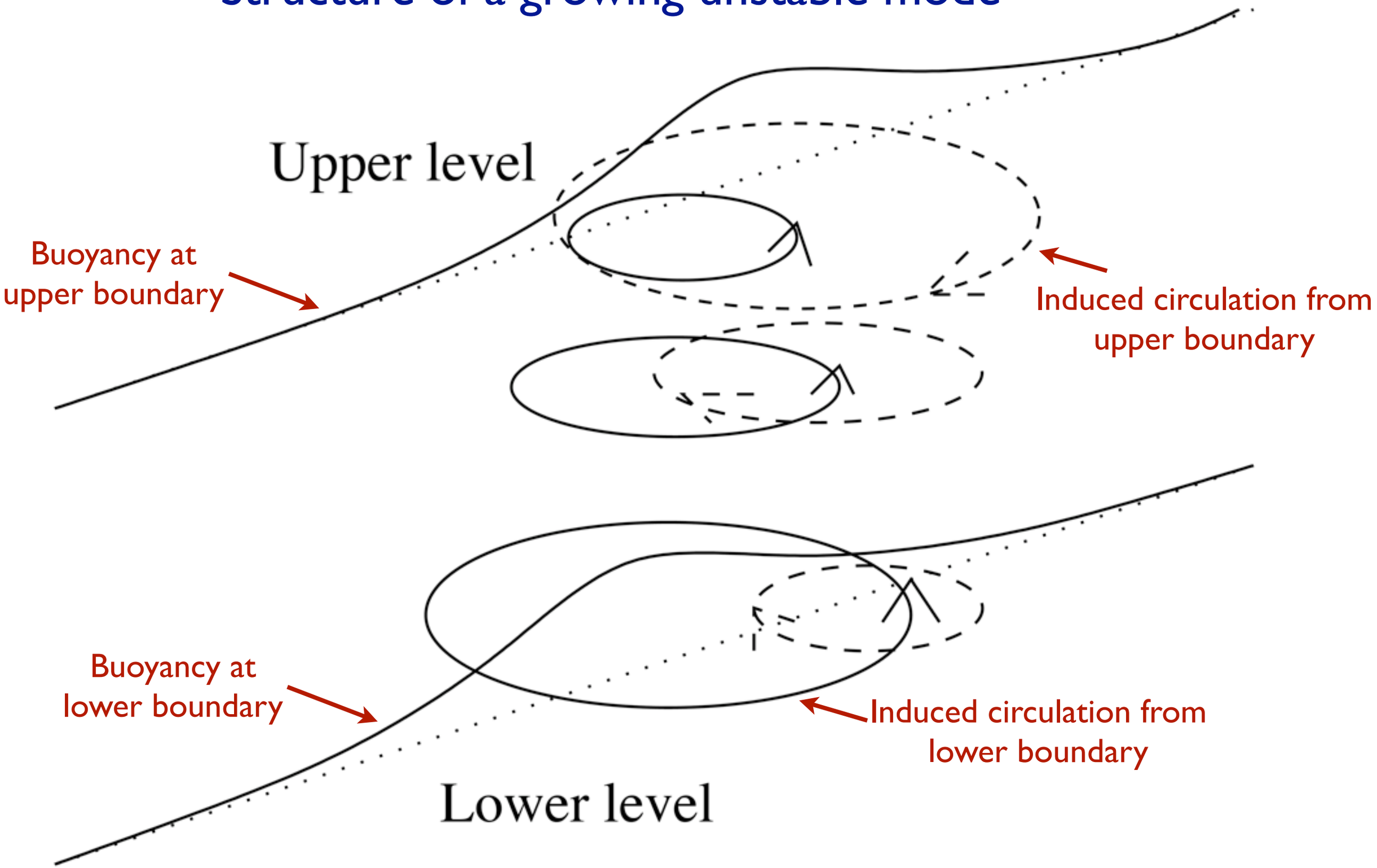

Fig. 7

Image courtesy of Glenn Flierl. Used with permission.

Structure of most unstable mode in the Eady model

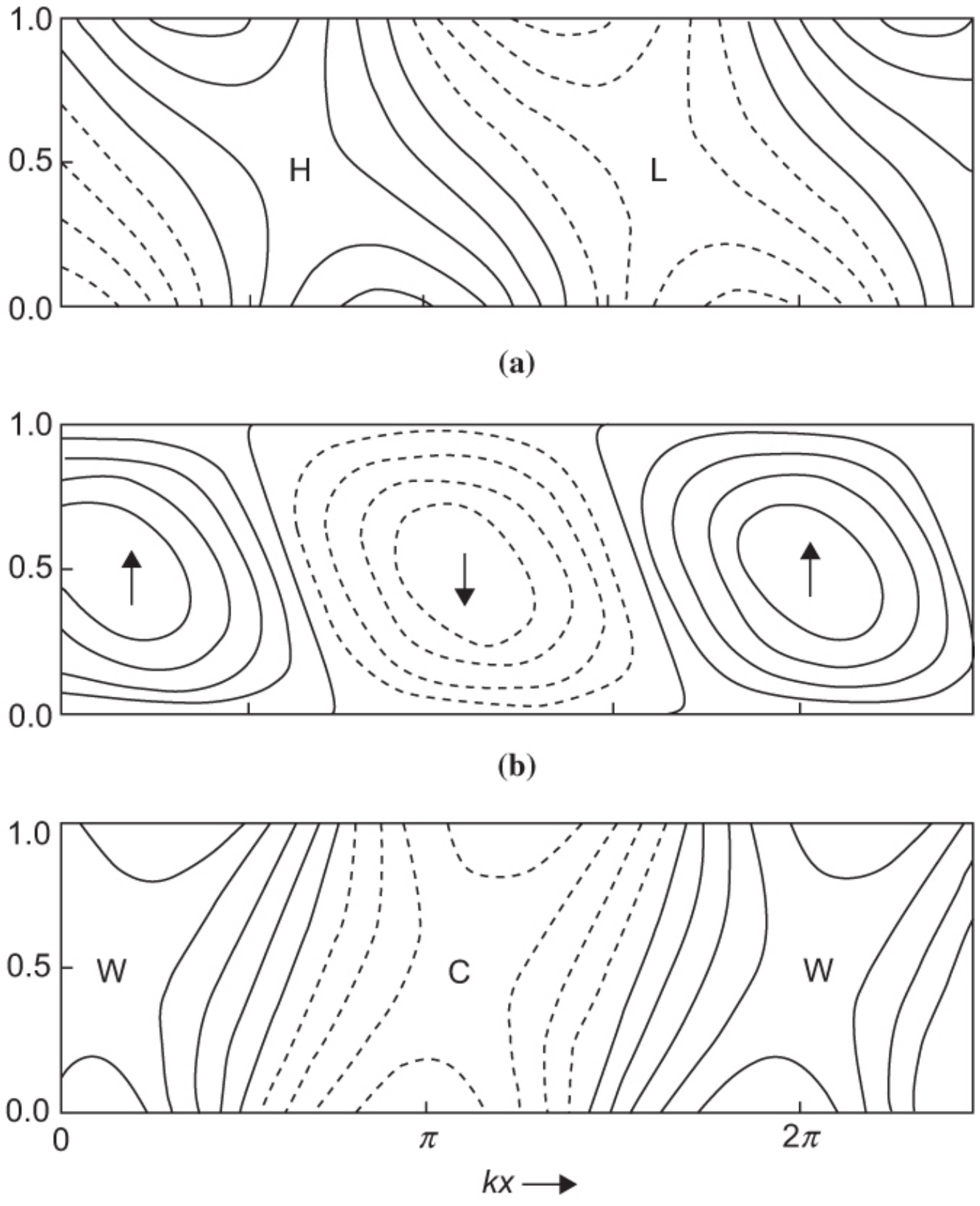

Perturbation geopotential height

Vertical velocity

Temperature

Fig. 8

Phase speed as a function of wavenumber in the Eady model

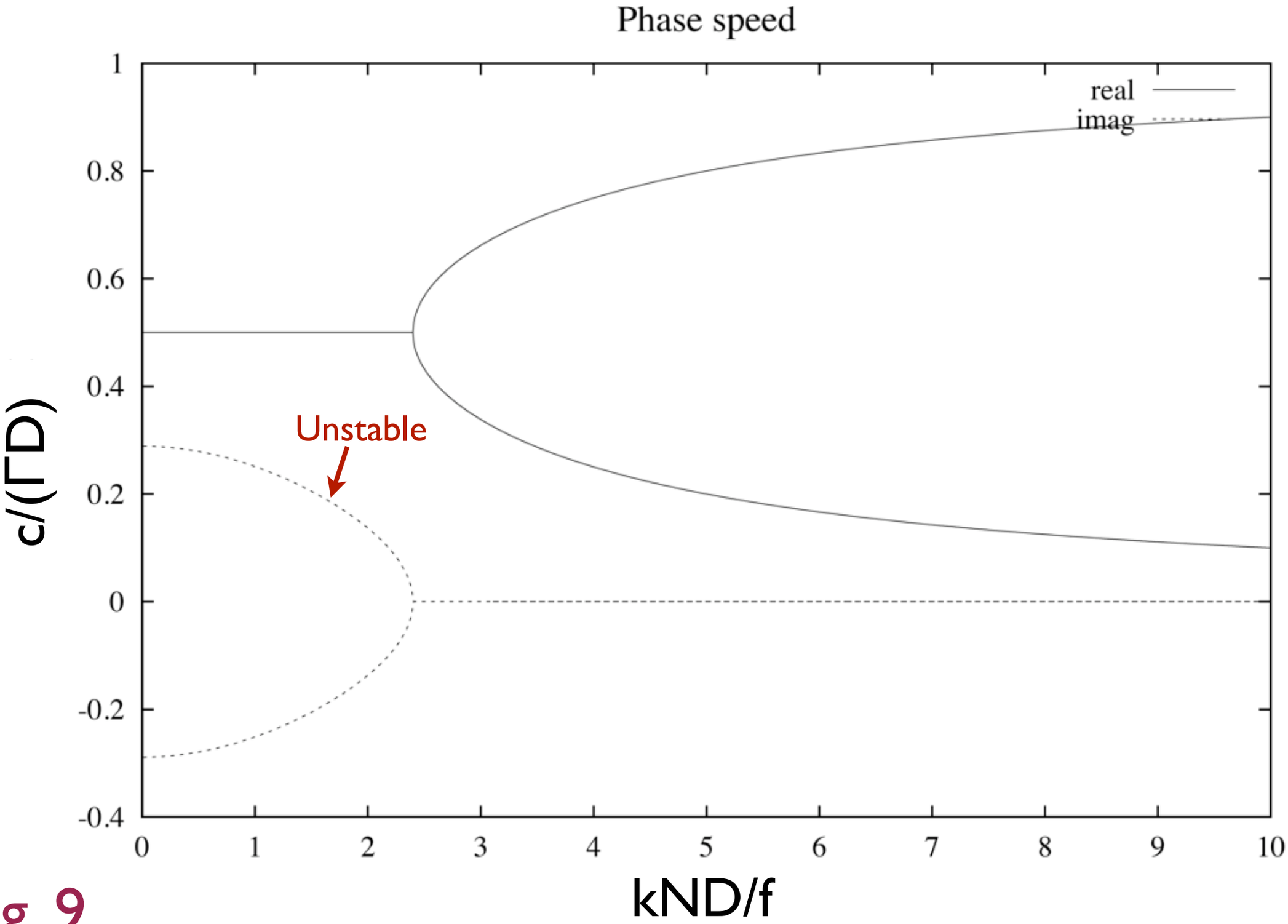

Fig. 9

Image courtesy of Glenn Flierl. Used with permission.

Kinetic energy of eddies is enhanced in "storm track" regions

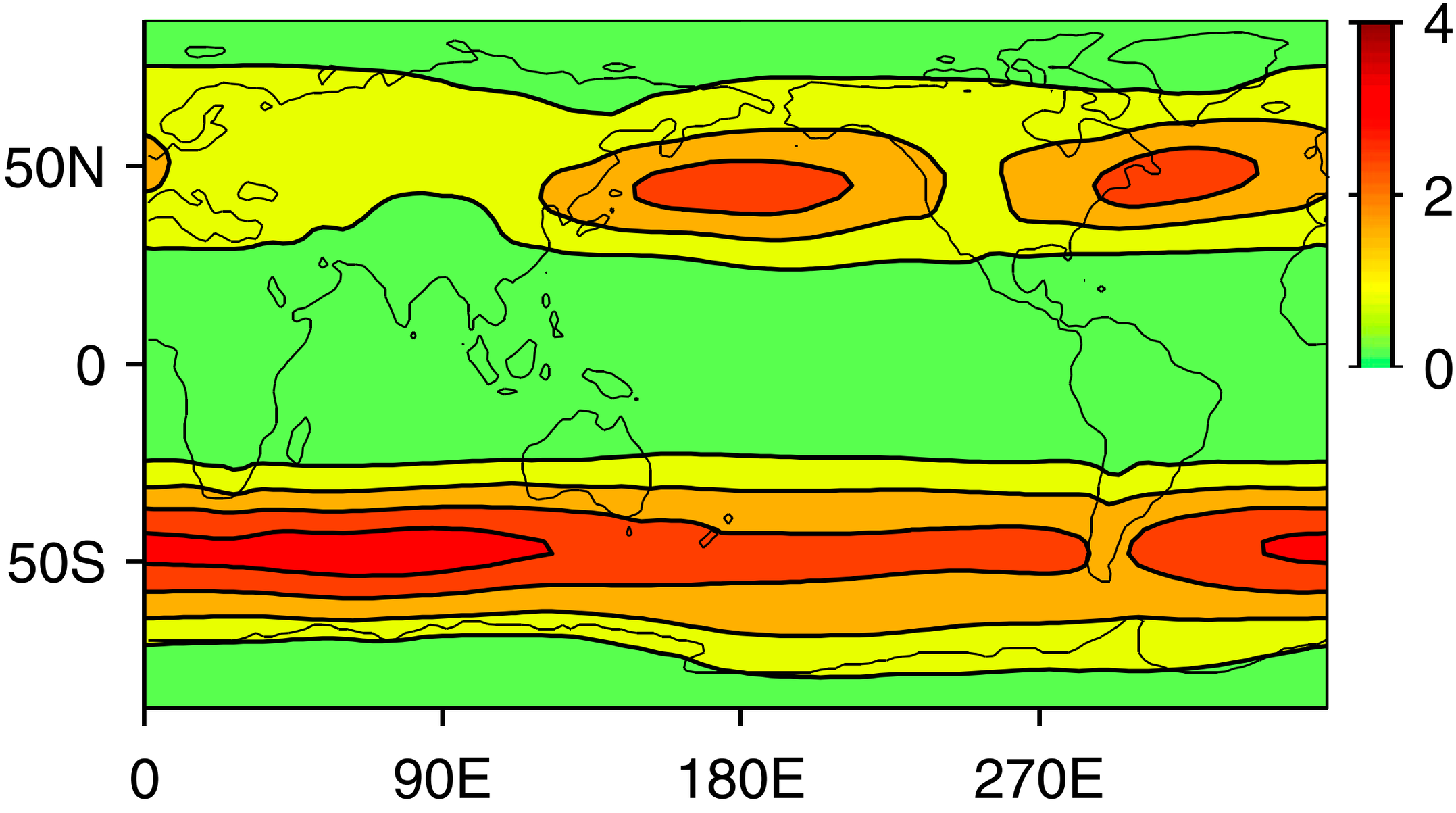

Eddy kinetic energy (10^5 J m^{-2}) based on high-pass filtered winds with a 6-day cutoff (figure based on GCM output)

Fig. 10

Can roughly identify storm track regions using maximum Eady growth rate

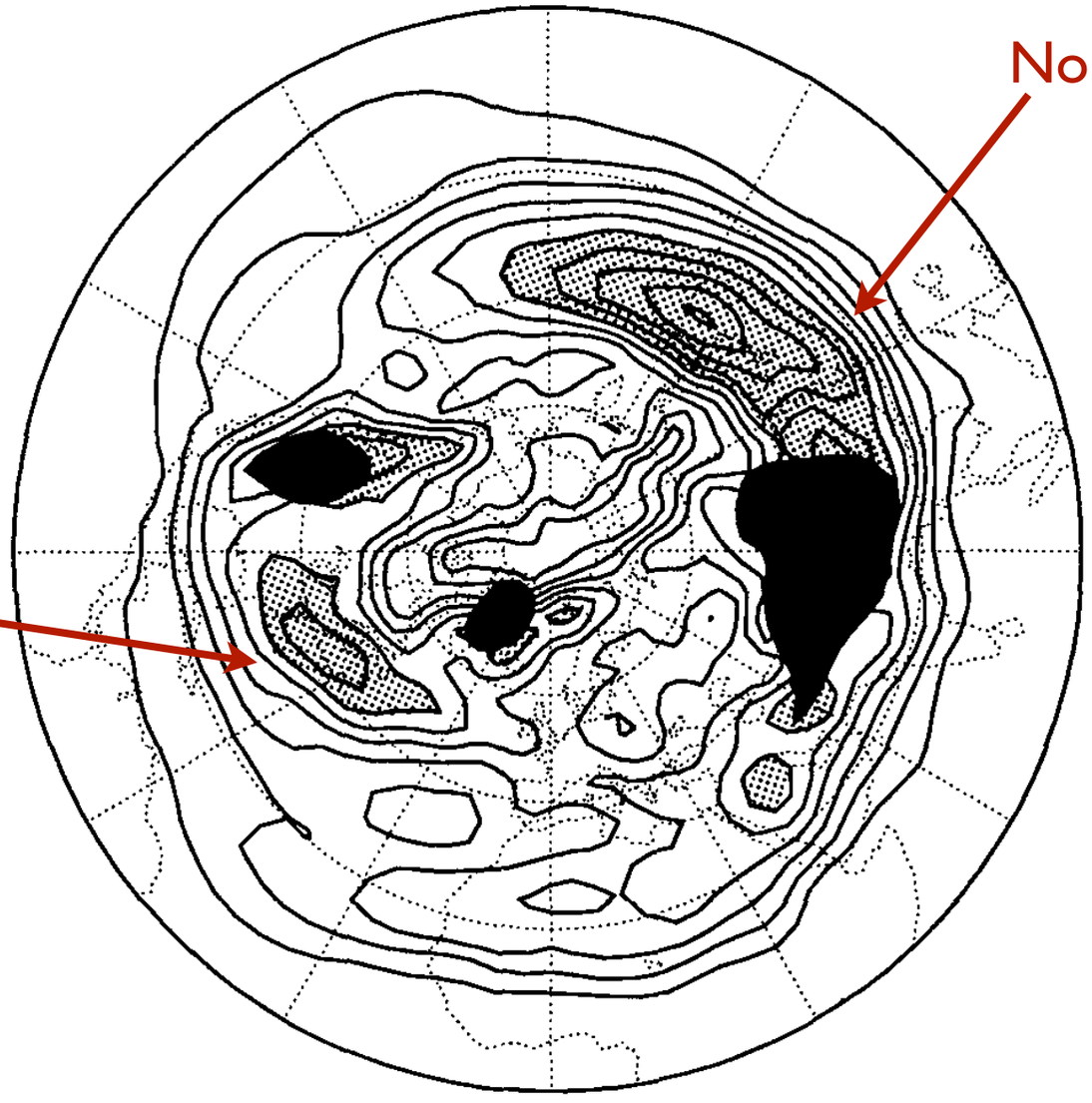

FIG. 2. The baroclinicity parameter $\sigma_{BI} = 0.31\ f|\partial v/\partial z|N^{-1}$ at about 780 mb for the Northern Hemisphere winter mean. The contours are drawn every 0.1 day^{-1} with zero at the equator and values below 0.1 day^{-1} at the North Pole. The stippling indicates values in excess of 0.6 day^{-1}. The region in which the 780 mb level is within 1 km of the orography and, therefore, probably in the boundary layer, is blacked.

Fig. 11

Hoskins & Valdes 1990

Cyclogenesis often involves pre-existing upper level PV anomaly

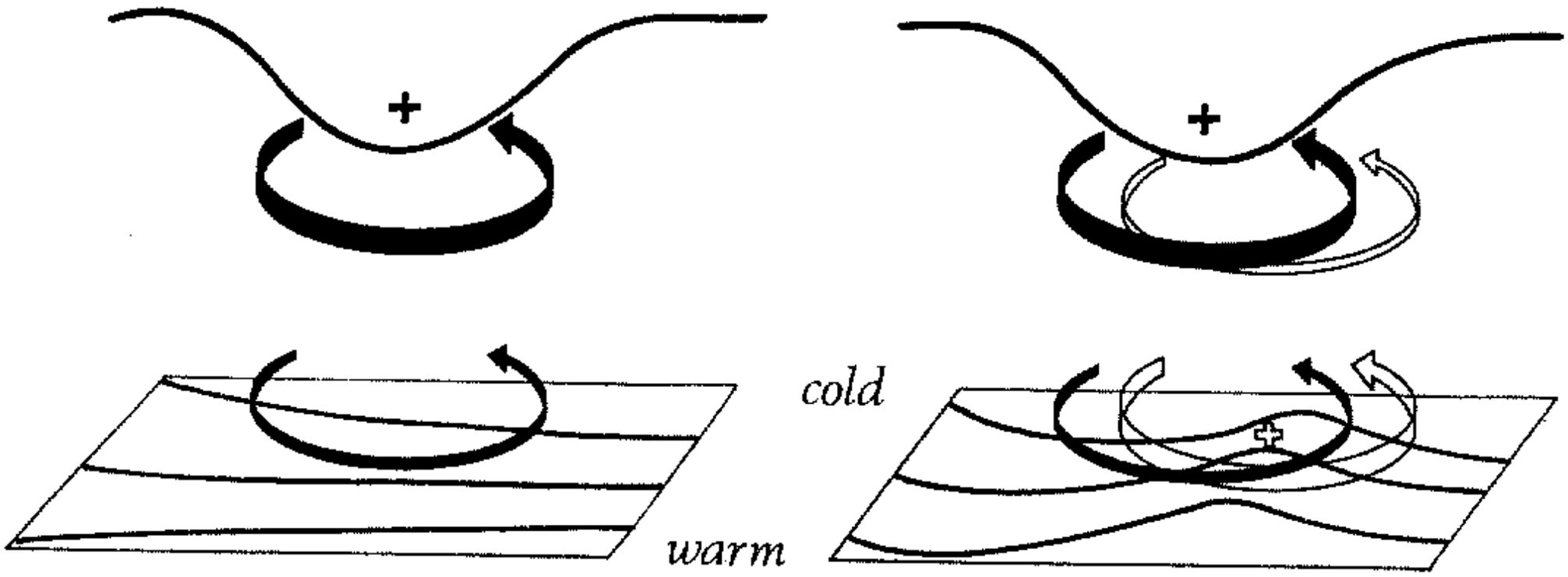

a b

Figure 21. A schematic picture of cyclogenesis associated with the arrival of an upper air IPV anomaly over a low-level baroclinic region. In (a) the upper air cyclonic IPV anomaly, indicated by a solid plus sign and associated with the low tropopause shown, has just arrived over a region of significant low-level baroclinicity. The circulation induced by the anomaly is indicated by solid arrows, and potential temperature contours are shown on the ground. The low-level circulation is shown above the ground for clarity. The advection by this circulation leads to a warm temperature anomaly somewhat ahead of the upper IPV anomaly as indicated in (b), and marked with an open plus sign. This warm anomaly induces the cyclonic circulation indicated by the open arrows in (b). If the equatorward motion at upper levels advects high-PV polar lower-stratospheric air, and the poleward motion advects low-PV subtropical upper-tropospheric air, then the action of the upper-level circulation induced by the surface potential temperature anomaly will, in effect, reinforce the upper air IPV anomaly and slow down its eastward progression. (To this extent the situation is similar to the small-amplitude instability situation represented by Fig. 18 and described in section 6(*b*).)

Fig. 12

Hoskins et al 1985

Example of cyclogenesis: Presidents day storm 1979

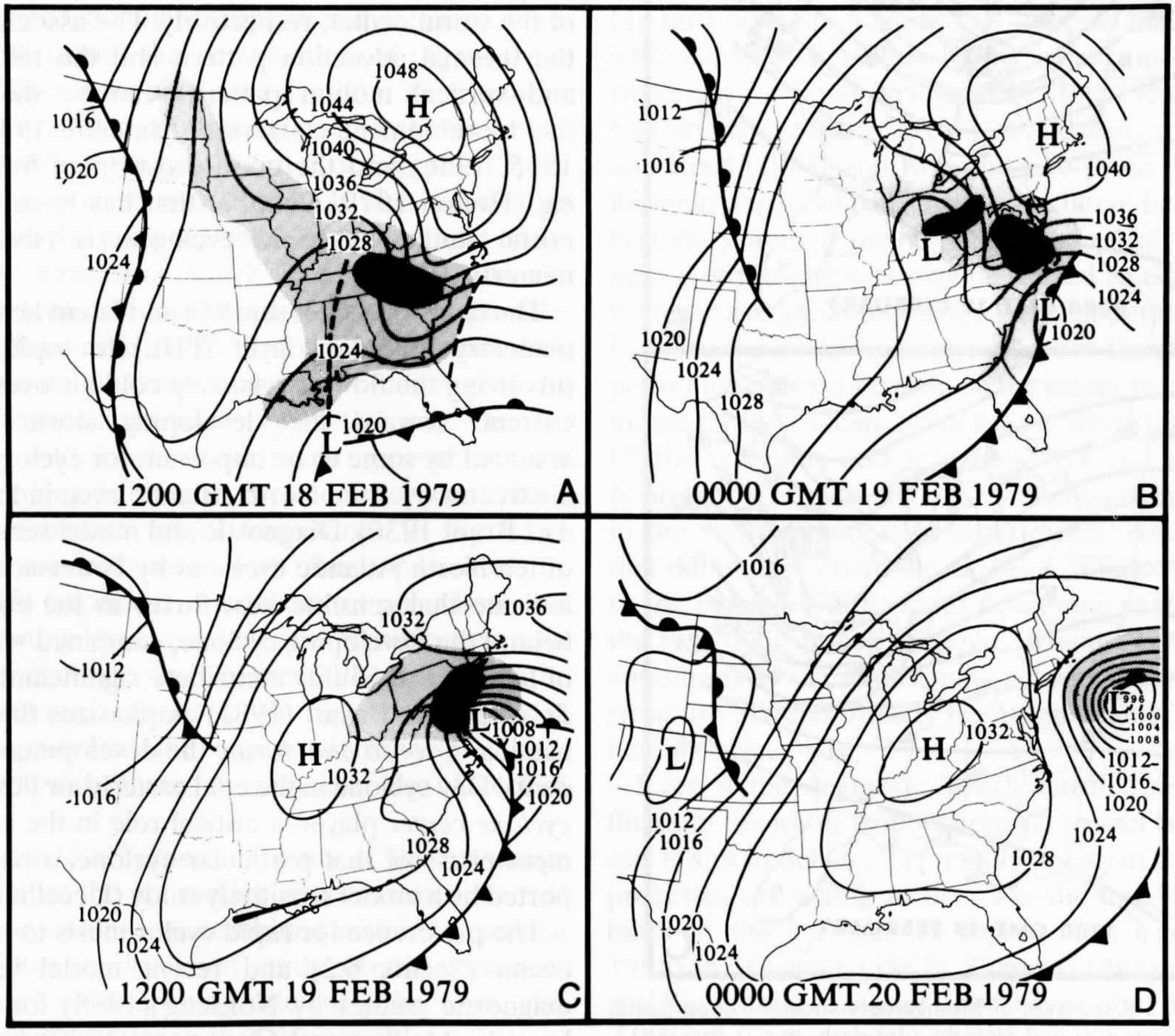

Fig. 13

FIG. 6.9. Sea-level pressure (mb) and surface frontal analyses for: (a) 12 UTC 18 February, (b) 00 UTC 19 February, (c) 12 UTC 19 February and (d) 00 UTC 20 February 1979. Shading indicates precipitation; dark shading, moderate to heavy precipitation. Dashed lines in (a) denote inverted and coastal troughs (Uccellini et al. 1985).

Example of cyclogenesis: Presidents day storm 1979

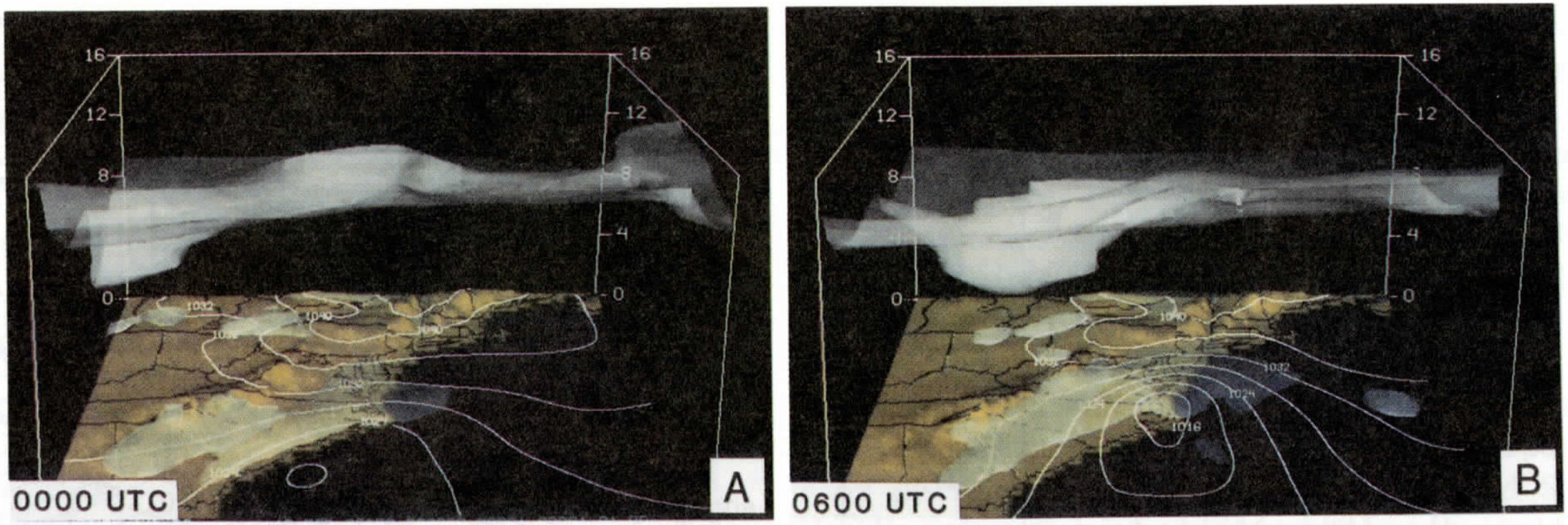

Fig. 13

FIG. 6.12. Three-dimensional perspectives, as viewed from the south, of the 2×10^{-5} K mb^{-1} s^{-1} IPV surface, and sea-level pressure isobar pattern (mb) derived from the numerical simulation of the Presidents' Day cyclone of Whitaker et al. (1988) for (a) 00 UTC, (b) 06 UTC, (c) 12 UTC and (d) 18 UTC 19 February 1979. The three-dimensional perspectives were derived by William Hibbard using the University of Wisconsin, Space Science and Engineering Center, three-dimensional McIDAS system.

Formation of fronts at lower and upper boundaries in Eady model with ageostrophic advection (semigeostrophic Eady model)

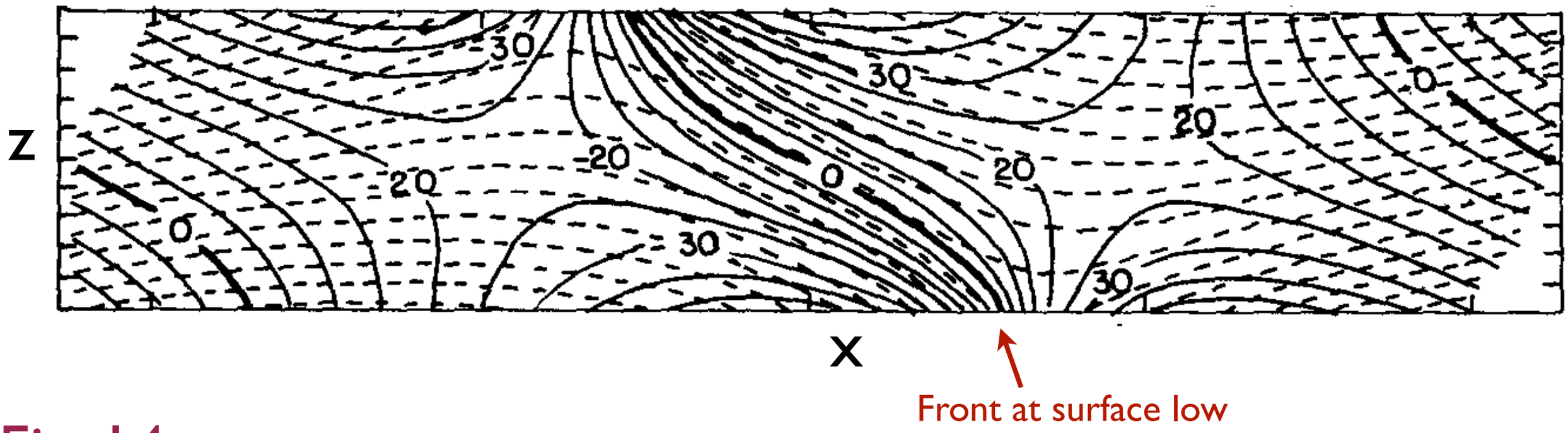

Fig. 14

Solid lines: Meridional velocity (contour interval 5 m/s)
Dashed lines: Potential temperature (contour interval 4K)

Emanuel, Fantini, Thorpe; 1987

12.810 Dynamics of the Atmosphere

Spring 2023